ARTICLE TYPE www.rsc.org/xxxxxx | XXXXXXXX

Wax-Based Microfluidic Chip and Its Application in One Step 3D Bonding

Xiuqing Gong,[a] Xin Yi[a], Kang Xiao[b], Shunbo Li[a], Rimantas Kodzius[c], Chih-kuan Tung[d], Jianhua Qin[e], Weijia Wen*[a, c]

Received (in XXX, XXX) Xth XXXXXXXXX 200X, Accepted Xth XXXXXXXXX 200X
First published on the web Xth XXXXXXXXX 200X
DOI: 10.1039/b000000x

We reported a simple, low-cost and detachable microfluidic chip incorporating easily accessible paper, glass slides or other polymer film as the chip materials along with adhesive wax as the reusable bonding material. We used a laser to cut through the paper or film to form channel and then sandwiched the paper and film between glass sheets or polymer membranes. The hot-melt adhesive wax can realize bridge bonding between various materials, for example paper, polymethylmethacrylate (PMMA) film, glass sheets, or metal plate. The bonding process is reversible and the wax is reusable through a melting and cooling process. With this process, one step formation of a three-dimensional (3D) microfluidic chip is achievable by vacuating the wax in a hot-water bath. To study the biocompatibility and applicability of wax-based microfluidic chip, we tested the PCR compatibility with the chip materials first. Then we applied the wax-paper based microfluidic chip to HeLa cell electroporation (EP). Subsequently, a prototype of 5-layer 3D microfluidic chip was fabricated by multilayer wax bonding. To check the sealing ability and the durability of the chip, green fluorescence protein (GFP) recombinant Escherichia coli (*E. coli*) bacteria were cultured. Chemotaxis of *E. coli* was studied in order to determine the influence of antibiotic ciprofloxacin concentration on the E. coli migration.

Introduction

Development in microfluidics has spurred growing interest in low-cost, straightforward and rapid prototyping of microfluidic devices. One of the most popular methods is soft-lithography which uses a soft polymer such as poly(dimethylsiloxane) (PDMS) to imprint and transfer the structure on a well patterned photoresistor [1-5]. PDMS, compared with other materials, has advantageous properties including typically low surface interfacial free energy, which enables it to conform to the surface of a master; an elastic characteristic, which allows it to be easily removed; and optical transparence, which improves transmission of UV and visible light. Although PDMS based microfluidic devices have been widely employed thanks to their ease of fabrication, there remain shortcomings. For example, PDMS absorbs small, hydrophobic molecules and the water evaporates through the PDMS film. Specifically, these effect microfluidic chip efficiency in that over long time durations, they compromise the cell culture media [6-9]. Another disadvantage of PDMS is the difficulty of constructing complex 3D structures by multilayer bonding; accompanying this usually requires a silane coupling agent to treat the PDMS surface, as well as laborious step-by-step bonding of the structures themselves [10, 11]. There is also the problem of the poor adhesion between metal and PDMS, making direct patterning of a conductive metal layer on the PDMS surface problematic [12]. An alternative rapid and inexpensive method of fabricating microfluidic chip is "print-to-cast" [13-21], for example the thermal pattern of wax. Methods in this area are mostly paper based microfluidic chips. Take the thermal printer-based chip fabrication method for example [14]. The process, utilizing a wax printer to directly pattern hydrophobic walls of wax in the hydrophilic paper, is less time consuming and less expensive. Morover, the hydrophobic pattern enables the biological fluid transport by means of capillary action in the millimeter sized porous cellulose. However, because the fluid can not form continuous flow in the paper, paper chip has many limitations, for example droplet cannot be formed by the paper chip, the liquid transport velocity depends on the passive capillary action and couldn't be actively changed, the cellulose fiber has absorption on many molecules, the chip is usually a open system and easy to be effected by ambient enviroment, and it is not easy to pattern electrode in cellulose network. As a result, paper chip is mostly used to develop simple, easy-to-fabricate, and inexpensive point-of-care chip for fast diagnostic application.

To complement the new functionalities and applications being developed in the microfluidic field, especially the conveted all-in-one system that is envisaged, a highly functionalized, ease-to-fabricate and low cost microfluidic chip is requried. In fact, opportunities abound, as there are many other types of inexpensive materials that can be utilized [22-26], materials that are both easily machinable [27], especially with mechanical or direct laser cutting technology [28-30], and inexpensive. A typical example is thin film or paper which are easily accessible in daily life as well, for example A4 paper (thickness: approximately 100 μm), transparent overhead-projector film, PMMA plates. However, the problem of how to bond them together quickly and effectively remains. The

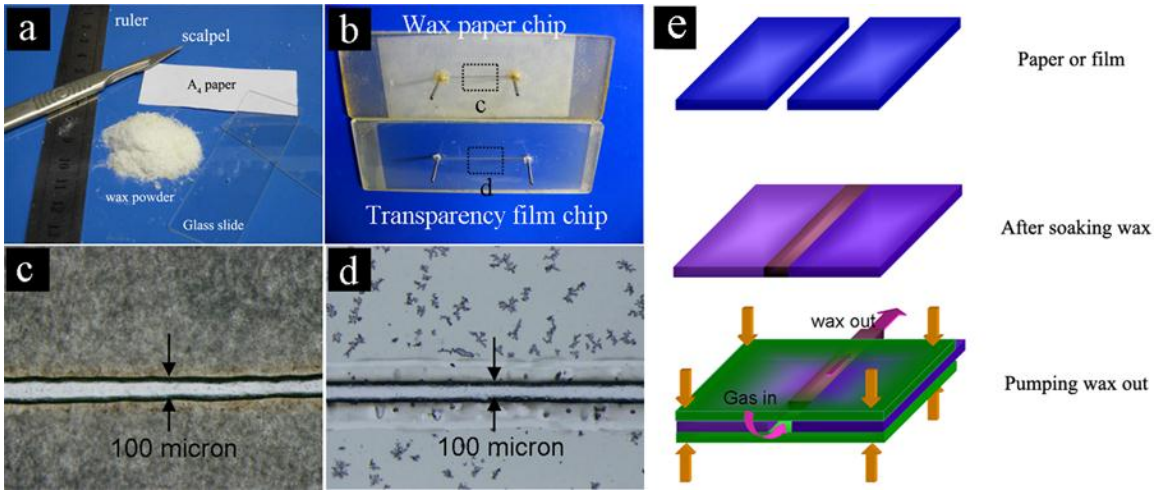

Fig. 1 (a) Materials required for simple 2D chip. A ruler and scalpel were used to align and cut the channel in the paper. Wax powder was used to fill the paper and bond it with glass slide. (b) Prototypes of paper-based chip (c) and film-based chip (d). (c) and (d) are magnified pictures corresponding to the selected area in (b). (e) Flow chat of chip bonding. After laser cutting, the paper or film absorbed wax at the wax's melting point. After cooling, the film or paper was sandwiched between two glass slides and immersed in a hot-water bath. The gas was introduced from the inlet to the outlet through which the wax in the channel was pushed

chip bonding materials that have been reported include adhesive glue bonding, solvent evaporation bonding, localized welding, or surface treatment and modification [31]. But glue and solvent bonding is restricted to specific materials, thermal fusion and welding bonding can not be applied to thin film (if < 100 μm), and surface modification usually require complex chemical treatment. Most recently, double-sided pressure sensitive adhesive (PSA) tape was introduced to chip bonding [15, 31]. Although this method is very cheap and convenient, the chemical composition of the adhesive is usually too complex for biological samples, the bonding strength is sensitive to environmental humidity and temperature, and bridge bonding between different materials (e.g. between glass and PMMA) is difficult. In this study, we proposed a hot melt bonding material and technology with which not only can different materials be reversibly bonded, but also one-step bonding of multiple layers together into 3D structure can be realized. The bonding material is a simple hydrocarbon alkyl based adhesive wax which can adhere to the material surface when melting. After cooling, adhesion is maintained without incident under exposure both to aqueous and solvent systems. The wax bonding, indeed, offers excellent bonding strength, and was designed to adhere to a wide range of substrates. In the semiconductor field, wax bonding normally is used to hold wafer in place during slicing, dicing, polishing and lapping process [32]. In the present study, we applied the wax bonding technology to microfluidic chip fabrication. We first evaluated the biocompatibility of materials employed in the chip fabrication, including PMMA, PC, paper and wax. To do it, we used polymerase chain reaction (PCR), one of the frequently used enzymatic reactions in microfluidics, as a model in an investigation of the PCR-inhibitory effect. To fabricate chip, we filled selected paper with melt wax and sandwiched it between different materials to form a wax-paper-based chip. Electrodes could be integrated into the chip for the purpose of HeLa cell electroporation. A prototype of 3D structure could be fabricated in a single step. We applied the 3D chip to a bacterial culture to test its sealing ability and durability. The chip also demonstrated a utility with a drug screening system designed to test the influence of drug concentration on the bacterial chemotaxis.

Methods

Laser cutting in different materials

We used a CO_2 laser (Versa Laser System, model VR3.50, Universal Laser Systems, Ltd.) to cut through thin-layer materials in continuous mode. The focal spot size is about 100 μm in width. The laser power varies from 5 W to 20 W and with the cutting velocity 0.76 mm/s. For example to cut through A4 paper, 5 watt power easily burns the paper and produces exact and uniform grooves along the entire length of the worked surface. The laser has been put to a wide range of uses in the field of organic soft matter. Such matter vaporizes to gaseous compounds upon laser cutting, and so a very clean cut can be performed [33, 34]. Intricate designs can be formed at high cutting velocity, without any stress or deformation of the organic film at 20 watt power. The channel dimension not only can be adjusted by varying the laser power of source, the scan speed, and the focus point, but depends also on the composition and thickness of the cut materials. For a 100 μm-thick A4 wood paper sheet, the smallest size obtainable is around 50 μm in width, whereas for 90 μm-thick transparent film, about 100 μm. For the purpose of the present study, the thin film materials employed included A4 wood paper acquired from FUJI XEROX (Japan), transparent film (Polypropene, about 90 μm in thickness as measured) obtained from 3M Company (USA), PMMA (1 mm in thickness) and polycarbonate (PC, 500 μm in thickness) membrane purchased from Techplast coated Product, Inc (USA).

Wax and wax bonding

The materials used in the preparation of microfluidic chips,

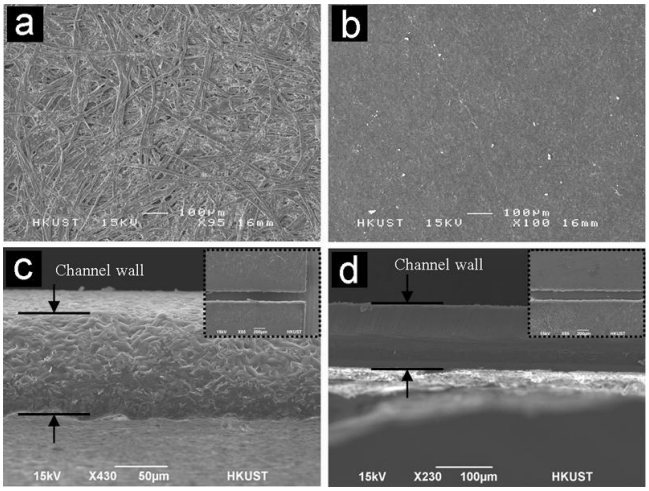

Fig. 2 (a) Surface morphology of A4 wood paper before absorbing wax, (b) after absorbing wax, (c) channel wall of wax-filled paper. (d) channel wall of transparent film. The inset pictures are the corresponding wax paper and transparent film channels.

shown in Fig. 1a, are easily accessible and inexpensive. For the paper-based chip, we first used a scalpel or laser to cut a channel in the paper, after which we let the paper absorb the hot-melt-type adhesive wax (purchased from NIKKA SEIKO [SKYWAX Series, Japan]) for 10 minutes at the melting point of wax. After cooling down, the wax paper was sandwiched between two glass slides in which inlet and outlet holes had been drilled (Fig.1b). These three layers were pressed together by four clamps at four corners and the bonding process was finished in a hot-water bath (70°C), using a syringe to control the gas pressure, which pressure slowly pushed out the wax (Fig. 1e). After rinsing it under cool water, the wax between the different layers solidified, enabling their adhesion. However, the resultant wax paper chip is opaque owing to the non-transparency of the paper. In order to make a transparent one, we substitute transparent film for the paper (Fig. 1b). Fig. 1c and d are the top views of the channels cut in the wax paper and transparent film. It can be seen that the channel edge made of the transparent film (Fig.1d) is sharper than in the wax paper (Fig.1c). That is because the surface of the paper channel is rougher and more porous. To make comparison, we scan the surface morphology of the paper and film by SEM. Fig. 2a shows the surface structure of the paper, which is interconnected by millimeter-sized cellulose. Fig. 2b shows the paper surface after having absorbed wax and being compressed by the glass slide. As is apparent, the surface became smooth, adhering tightly to the glass slide. Fig. 2c and d are the surface morphology of the paper and film channel wall. Clearly, the channel wall cut into the wax paper is rougher than that in the transparent film, which corresponds to Fig. 1c and d.

3D microfluidic chip

Wax bonding can also be applied to the fabrication of complex 3D structures in different materials. A prototype of a 3D microfluidic chip was shown in Fig. 3, The chip is composed of 5 layers of which the 1st and 5th layer are 1 mm-thick pyrex glass slides, the 2nd and 4th layer are 1 mm-thick

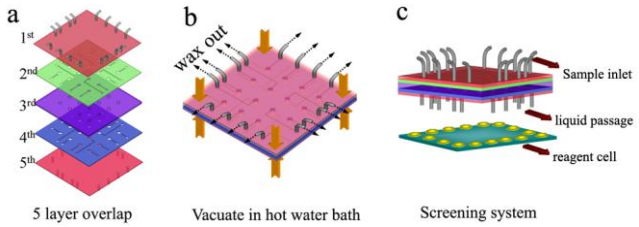

Fig. 3 (a) 5 layers were overlapped and aligned. The 1st and 5th layer are glass slides, the 2nd and 4th layer were 1mm thick PMMA, and the 3rd layer was 500 μm-thick PC. All of the layers were wetted by melt wax before being overlapped. (b) Layers were pressed together by four clamps at four corners (yellow arrows). The prototype device was immersed in a hot-water bath and then set in a vacuum chamber to evacuate the wax from the chip through the channel. (c) Structure of bacterial screening system comprised of upper screening chamber and lower reagent cell. The liquid passage was glass capillary which allowed the movement of liquid by capillary action.

PMMA, and the 3rd layer is 500 μm-thick PC (Fig. 3a). Holes had been drilled in the glass slides for the purpose of inlet and outlet which were connected by steel tubes (sample inlet, 1 mm in dimension) and glass capillaries (liquid passage, 1 mm in dimension). The 3rd layer was a 4 × 4 array for screening chamber. The width of the chamber is 2 mm. On both sides of the 3rd layer are the channel layers (2nd and 4th), which is to guide the flow of liquids and lead them to the screening chambers. The channel is 200 μm in width. They all were formed by laser-cutting through the thin materials with 20 watt power. Preparatory to the assembly of the layers, the PMMA and PC layers were immersed in melt wax. After cooling, the five layers were overlapped and well aligned before being placed in a vacuum oven (SHEL LAB, USA). Four clamps were used to hold all of the layers together at their four corners (yellow label in Fig. 3b). Then, the assembly was immersed in a hot-water bath (70°C) and vacuated. After venting and evacuating the assembly several times, the wax in the channels was pushed out of the chip, after which it floated to the surface of bath, because of lower density than water. A reagent cell was also fabricated by laser cutting in the PMMA board. The width of the cell is 1.5 mm. The structure of the 3D screening system is shown in Fig. 3c.

Materials investigated

The following materials were first tested for enzymatic compatibility: PMMA, PC, pyrex glass, A4 printing paper, wax and paper impregnated with the wax. The materials were manually broken into small fragments and a sample of size >5 mm^2 to each PCR reaction tube was added (see the supplemantary information).

Material enzymatic biocompatibility

A large number of materials, including silicon, glass, various plastics and others, currently are used in microfluidics chip production. When these materials come in contact with biomolecular reaction components, adsorption and inhibition of biomolecules arise as problems to be avoided [35, 36]

In this study, we first accessed material biocompatibility by testing the absorption of DNA and protein on chip materials. Biocompatibility of materials can be measured on DNA,

RNA,

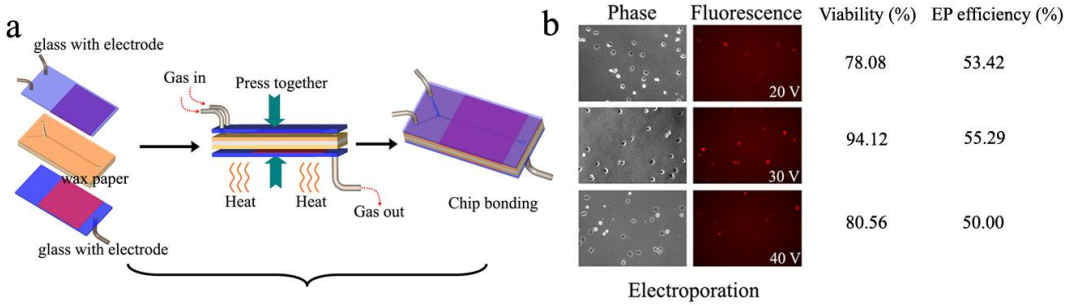

Fig. 4 (a) The flow chart to show the fabricating process of a wax-paper-based microfluidic device with imbedded electrodes. (b) The images of cells under bright field and fluorescent field. The cell viability and the EP efficiency are also presented.

protein (enzymatic) or cellular level. PCR reaction contains both DNA and enzyme (polymerase). Therefore we chosen PCR for material biocompatibility testing. PCR mix incubated with materials but without BSA provided clues as to which materials are PCR-inhibitory. Most bio-friendly materials exhibit similar signals regardless of the inclusion or not of BSA in the PCR mix: these are PMMA, PC and pyrex glass and wax. The signal is comparable to the no additive control's (Fig. S1). Wax is inert, and as such, does not expect to interact with PCR components. Wax is even until now used to cover PCR mixtures and avoid evaporation. No signal was obtained in PCR mix incubated with paper despite BSA inclusion. Interestingly, a signal was obtained in PCR including paper impregnated with the wax with the addition of BSA. The signal strength was similar to the PCR with included wax material. The results show that wax impregnated paper behaves differently than the pure paper by avoiding PCR-inhibitory and should be biocompatible with enzymes.

Wax paper chip for electroporation

Electroporation has been used as a powerful cell transfection method which is to deliver membrane-impermeable macromolecules into cells [37, 38]. The advantage of on-chip electroporation is a small quantity of samples and an uniform electric field in these narrow regions, which helps enhance both cell viability and EP efficiency with few side effects that are known to exist in the conventional devices [39-43]. Wax bonding provides an effective way of metal bonding and electrode imbedding. To test the uniformity of electric field, we sputtered 10 nm-thick gold onto glass slides as cover and lower layer, and sandwiched wax paper between to bond them together.

The chip bonding process is shown in Fig. 4a. Both the channel width and depth were 100 μm. The planar electrode area is 100 μm in width and 2 cm in length. We performed experiment of red dye untake into HeLa cells for various electric fields generated in the channel. HeLa cells obtained from American Type Culture Collection (ATCC, Manassas, VA) were suspended in the poration medium containing dextran, rhodamine B isothiocyanate, 70S (R-9379) purchased from sigma, and then filled into one channel. The density of the cells in the poration medium was about 10^5 cells/ml. The volume of the mixture in the electrode area was about 0.2 μl. The sample volume was controled by syringe pump. We blew N_2 gas into another channel to push the sample. The electrodes were connected to a radio-frequency (RF)-oscillating electric pulse generator (Bio-Rad Labs). Two trains of electric pulses were applied to the cell/dye mixture suspension at 10 second intervals. The waveforms of the output electric pulses were monitored using a digital storage oscilloscope (Tektronix 2221A). There're 10 pulses in each train. The frequency is 30 kHz, duration time of each pulse is 5 ms and interval between each pulse is 100 ms. After applying different voltages, the cells under bright and fluorescent field were counted. The viability as well as EP efficiency was listed as shown in Fig.4b. Applying 30 volt to the electrodes could get better viability as well as EP efficiency than 20 volt and 40 volt. The mean viability is 84.25 ± 8.63 %, accompanying with the EP efficiency 52.91 ± 2.68 %. The result first indicates the wax can be utilized to bond metal electrodes with chip together. Second, there is no liquid leakage appearing in the channel even after repeated usage. This means that the wax has good sealing ability which can hold different materials together. Third, we didn't see cell trapping phenomenon in the chip which suggests that the wax has no absorption on the cells during the EP process. The wax-bonded electrodes can also be applied to other electro-dynamic process, for example electrophoresis, or on chip electro-detection.

3D chip for bacterial culture and screening

To test the durability of the wax bonded 3D microfluidic chip (Fig. 3), we applied it to the culture and screen of GFP (Green fluorescence protein) recombinant *E. coli* bacterial. Fig. 5a is the top view of the transparent chip. Fig. 5b shows the flow line of liquid in the 3D chip as we infused red dye solution to the chip. The chemotactically wide type *E. coli* strain was a motile strain with RP437 transformed with a high copy plasmid expressing ampicillin resistance and GFP expression. To culture the *E. coli*, we first infused the standard growth medium L-Broth to the sixteen screening chambers from the sample inlet (Fig. 3c), one liter of medium containing 10 g of tryptone, 5 g of yeast extract, 10 g of sodium chloride, and 2

ml of ampicillin solution (100 mg/ml). One *E. coli* bacterial colony on agar plate was transfered to the tube with 3 ml L-

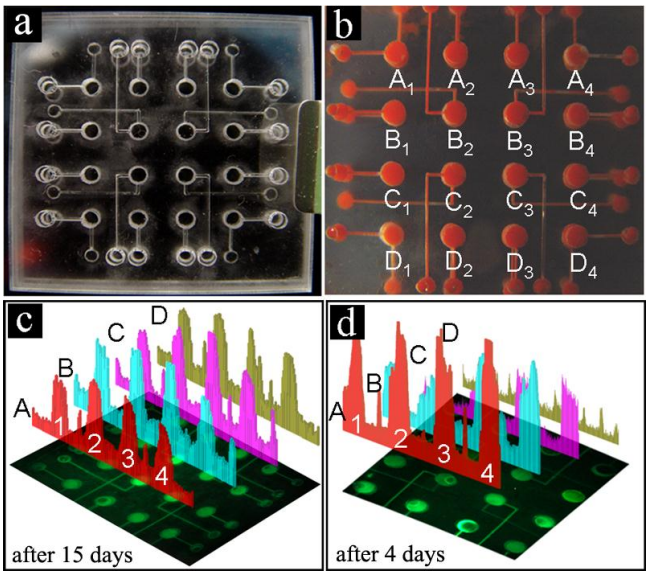

Fig. 5 (a) Top view of 5-layer 3D structure, (b) Red dye solution was infused to indicate screening chambers, (c) GFP recombinant *E. coli* bacteria were cultured in screening chambers showing green fluorescence protein. The peak appears at the row A, B, C, and D labeled by digits 1, 2, 3, and 4 is to show the intensity of fluorescence corresponding to the screening chamber beneath them, (d) The chemotaxis phenomenon of *E. coli* bacteria responding to the antibiotic concentration.

Broth and 10 μm amiciline. The tube was incubated and shaked at 30 ^{o}C for 6 hours. One droplet of the bacterial broth was added to the 16 reagent cells. Then, the liquid passage of the screening device was inserted into the reagent cell. The *E. coli* bacteria migrated through the glass capillary to the screening chamber full of food resources, where they proliferated and expressed strong green fluorescence. The GFP labeled bacteria were imaged by an inverted fluorescence microscope (Axiovert 200M, Zeiss) equipped with a cooled CCD camera (Diagnostic Instruments). The full-range-picture was taken by a Canon camera (EOS 5D, Mark II) equipped with a macro lens (MP-E, 1-5×). The image data acquired from the CCD camera were further processed and analyzed by MetaMorph (Universal Imaging Corp.). Quantitative analysis was carried out with the help of Excel (Microsoft), and refined images were done by Confocal Assistant v4.0 (Bio-Rad) and Adobe Photoshop. The motion of cells upwards from the reagent cells to the food-enriched screen chambers occurred as all the channels were full of fluorescence which interacted through chemotactic signaling in bacterial system [44, 45]. Eventually, at about 15 days all of the chambers are full of GFP fluorescence. The fluorescent images and the fluorescence intensity measurement (Fig. 5c, A, B, C, and D) indicate that the bacteria underwent a uniform rate of proliferation throughout the chambers. The *E. coli* bacteria recovered motility after we detached the chip and cultured them again in the tube. The result proved that the 3D microfluidic chip could endure long time bacterial culture without liquid leakage even after 15 days incubation, and the screening system is enviromental to the bacterial culture.

To demonstrate the drug screen performance, we added different concentrations of antibiotic solution to the reagent cells. The chemotactically antibiotic solution used was

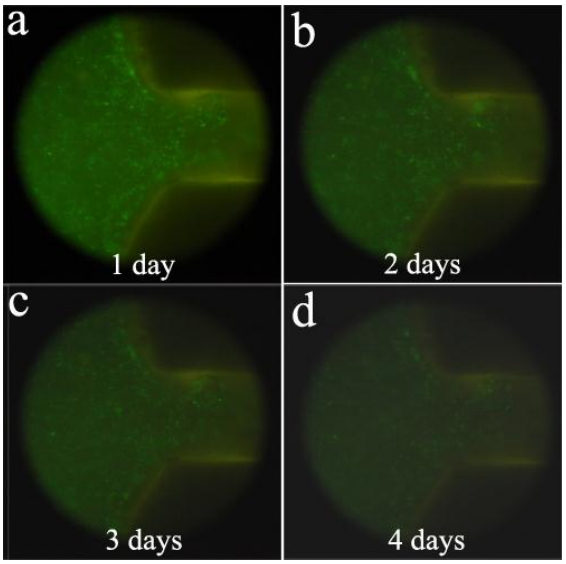

Fig. 6 The *E. coli* bacteria migrate out of chip after (a) 1 day, (b) 2 days, (c) 3 days, and (d) 4 days.

ciprofloxacin, because ciprofloxacin doesn't kill *E. coli* while can stop the multiplication of *E. coli* by inhibiting the reproduction and repair of the genetic material [46]. To prepare the antibiotic solution, we dissolved 10 mg ciprofloxacin power into 1 ml water and used hydrochloride acid to adjust the pH value at 3.5. We diluted it to different concentrations and infused them in reagent cells. After that, the capillary tubes were immersed in the antibiotic solution to study the chemotactical phenomenon. After 4 days, the fluorescence intensity decreased with the increasing of the ciprofloxacin concentration in the reagent cell. Specifically, almost all the *E. coli* bacteria migrated out of the chamber of C1 (800 ng/ml), C2 (700 ng/ml), D1 (1200 ng/ml), D2(1100 ng/ml), D3 (1000 ng/ml), and D4 (900 ng/ml) as shown in Fig. 5d; a few amount of bacteria move out of the chamber of B1 (400 ng/ml), B2 (300 ng/ml), C3 (600 ng/ml) and C4 (500 ng/ml); there is no obvious change in the chamber of A1 (no ciprofloxacin), A2 (10 ng/ml), A3 (20 ng/ml), A4 (30 ng/ml), B3 (100 ng/ml), and B4 (200 ng/ml). Fig. 6 shows the relationship of bacterial motion versus time in chamber C2. It was clearly seen that after 4 days incubating most of the bacteria moved out of the chambers upwards to the channels and sample inlets. The drug screening result proves that the wax bonded 3D chip has no influence on antibiotic molecules and can resist acidic condition. The wax-bonded 3D chip also has good optical transparence and could be applied to other optical analysis methods in the future research.

Conclusions

We reported a low-cost and detachable microfluidic chip utilizing easily accessible paper, glass slides or other thin material as the basic materials along with hot-melt wax as the reversible bonding material. The chip fabrication process is

simple by controlling the temperature and the gas pumping pressure. The melt wax in the channel is easily pushed out of the chip by gas or vacuation, while the other wax, sandwiched between the materials, is retained so as to play its key role in chip bonding after post-cooling. Laser cutting technology was used to cut through the paper or film to form a channel. The paper or film was then sandwiched between glass sheet or polymer membrane where the wax could form bonding between the various materials, such as PMMA, PC, glass sheet, or metal plate. The wax-based chip is detachable in so far as the bonding process is reversible by means of re-melting the wax. We first used the PCR to test the biocompatibility of chip materials with DNA and protein. Subsequently, a microfluidic chip prototype incorporating bonded metal thin layers as electrodes was fabricated. The applicability of the electrodes was tested by subjecting them to HeLa cell electroporation. The influence of voltage on the electroporation efficiency was determined by comparing the cells of bright field phase with the fluorescence phase. With this technology, a three-dimensional (3D) microfluidic chip is achievable in one step at last. We were able to overlap 5 layers of different materials together and vent and vacuate it in a hot-water bath. After repeating these two steps several times, the wax in the channel was pushed out of the chip, floating to the surface of the water bath. The original channel was then filled with water in order to avoid the blockage of the channel after cooling. To test the sealing ability and durability of the 3D microfluidic chip, GFP recombinant *E. coli* bacteria were cultured in 4×4 screening chambers. After 15 days of incubation, the bacteria maintained their fluorescence, and they recovered their motility after culturing them again in the tube. Thereby, it was proved that the wax-bonded chip has good sealing ability, durability and effective biocompatibility over long cell culture periods. The 3D chip is transparent and can also be applied to drug screening. We added different concentrations of antibiotic ciprofloxacin to the cell reagent to stop the multification of *E. coli* and study the chemotaxis of the *E. coli* versus time. The screening image indicates that the *E. coli* bacteria could migrated through the channel without being absorbed by the wax or channel wall. The 3D device offers good optical transparency and low background fluorescence, making it applicable to optical detection on-chip.

Notes and references

[a] *Department of Physics, The Hong Kong University of Science and Technology, Clear Water Bay, Kowloon, Hong Kong. E mail: phwen@ust.hk*

[b] *Department of Biology, The Hong Kong University of Science and Technology, Clear Water Bay, Kowloon, Hong Kong.*

[c] *KAUST-HKUST Micro/Nanofluidic Joint Laboratory, The Hong Kong University of Science and Technology, Clear Water Bay, Kowloon, Hong Kong.*

[d] *Dalian Institute of Chemical Physics, Chinese Academy of Sciences, 457, Zhongshan Road, 11603, China.*

† Electronic Supplementary Information (ESI) available: [PCR biocompatibility with materials]. See DOI: 10.1039/b000000x/

1 Y. Xia, G. M. Whitesides, *Annu. Rev. Mater. Sci*, 1998, 28, 153.
2 J. C. McDonald, D. C. Duffy, J. R. Anderson, D. T. Chiu, H. Wu, O. J. A. Schueller, G. M. Whitesides, *Electrophoresis*, 2000, 21, 27.
3 Y. Xia, G. M. Whitesides, *Angew. Chem., Int. Ed.*, 1998, 37, 550.
4 D. Duffy, J. McDonald, O. Schueller, G. M. Whitesides, *Anal. Chem.*, 1998, 70, 4974.
5 X. Zhao, Y. Xia, G. M. Whitesides, *J. Mater. Chem.*, 1997, 7, 1069.
6 R. Mukhopadhyay, *Anal. Chem.*, 2007, 79, 3248.
7 M. W. Toepke, D. J. Beebe, *Lab Chip*, 2006, 6, 1484.
8 Lee, J. N., Park, C., Whitesides, G. M., *Anal. Chem.*, 2003, 75, 6544.
9 Y. S. Heo, L. M. Cabrera, J. W. Song, N. Futai, Y. C. Tung, G. D. Smith, S. Takayama, *Anal. Chem.*, 2007, *79*, 1126.
10 J. R. Anderson, D. T. Chiu, R. J. Jackman, O. Cherniavskaya, J. C. McDonald, H. Wu, S. H. Whitesides, G. M. Whitesides, *Anal. Chem.*, 2000, 72, 3158.
11 Y. Luo, R. N. Zare, *Lab Chip*, 2008, 8, 1688.
12 H. S. Chuang, S. Wereley, *J. Micromech. Microeng.*, 2009, 19, 045010.
13 E. Carrilho, A. W. Martinez, G. M. Whitesides, *Anal. Chem.*, 2009, 81, 7091.
14 Y. Lu, W. Shi, L. Jiang, J. Qin, B. Lin, *Electrophoresis*, 2009, 30, 1497.
15 G. V.Kaigala, S. Ho, R. Penterman, C. J. Backhouse, *Lab Chip*, 2007, 7, 384.
16 A. W. Martinez, S. T. Phillips, G. M. Whitesides, *PNAS*, 2008, 105, 19606.
17 X. Li, J. Tian, T. Nguyen, W. Shen, *Anal. Chem.*, 2008, 80, 9131.
18 A. W. Martinez, S. T. Phillips, E. Carrilho, S. W. Thomas, H. Sindi, G. M. Whitesides, *Anal. Chem*, 2008, 80, 3699.
19 A. W. Martinez, S. T. Phillips, M. J. Butte, G. M. Whitesides, *Angew. Chem. Int. Ed.*, 2007, 46, 1318.
20 S. K. Sia, V. Linder, B. A. Parviz, A. Siegel, G. M. Whitesides, *Angew. Chem. Int. Ed.*, 2004, 43, 498.
21 Y. Lu, W. Shi, J. Qin, B. Lin, Anal. Chem., 2010, 82, 329.
22 M. A. Witek, M. L. Hupert, D. S. Park, K. Fears, M. C. Murphy, S. A. Soper, *Anal. Chem.*, 2008, 80, 3483.
23 J. S. Buch, F. Rosenberger, W. E. Highsmith, C. Kimball, D. L. DeVoe, C. S. Lee, *Lab Chip*, 2005, 5, 392.
24 J. P. Rolland, R. M. V. Dam, D. A. Schorzman, S. R. Quake, J. M. DeSimone, *J. Am. Chem. Soc.*, 2004, 126, 2322.
25 V. I. Vullev, J. Wan, V. Heinrich, P. Landsman, P. E. Bower, B. Xia, B. Millare, G. Jones, *J. Am. Chem. Soc.*, 2006, 128, 16062.
26 S. Metz, R. Holzer, P. Renaud, *Lab Chip*, 2001, 1, 29.
27 D. A. Bartholomeusz, R. W. Boutté, J. D. Andrade, Journal of microelectromechanical system, 2005, 14, 1364.
28 H. Klank, J. P. Kutter, O. Geschke, *Lab Chip*, 2002, 2, 242.
29 H. Liu, H. Gong, *J. Micromech. Microeng.*, 2009, 19, 037002.
30 O. Rötting, W. Röpke, H. Becker, C. Gärtner, *Microsystem Technologies*, 2002, 8, 32.
31 R. T. Kelly, A. T. Woolley, *Anal. Chem.*, 2003, 75, 1941.
32 P. K. Yuen, V. N. Goral, *Lab Chip*, 2010, 10, 384.
33 H. Wada, H. Sasaki, T. Kamijoh, *Solid-State Electronics*, 1999, 43, 1655.
34 I. A. Choudhury, S. Shirley, *Optics & Laser Technology*, 2010, 42, 503.
35 M. A. Shoffner, J. Cheng, G. E. Hvichia, L. J. Kricka, P. Wilding, Nucleic Acid Res., 1996, 24, 375.
36 P. Wilding, M. A. Shoffner, L. J. Kricka, Clin. Chem, 1994, 40, 1815.
37 S. Baron, J. Poast, D. Rizzo, E. McFarland, E. Kieff, *J. Immunol. Meth.*, 2000, 242, 115.
38 U. Čegovnik, S. Novaković, *Bioelectrochemistry*, 2004, 62, 73.
39 M. Golzio, J. Teissié, M. P. Rols, *PNAS*, 2002, 99, 1292.
40 Y. Huang, B. Rubinsky, *Biomed. Microdev*, 1999, 2, 145.
41 Y. Huang, B. Rubinsky, *Sens. Actuators A*, 2001, 89, 242.
42 Y. Huang, B. Rubinsky, *Sens. Actuators A*, 2003, 104, 205.
43 T. Tsukamoto, N. Hashiguchi, S. M. Janicki, T. Tumbar, A. S. Belmont, D. L. Spector, *Nature Cell Biol.*, 2000, 2, 871.
44 S. Park, P. M. Wolanin, E. A. Yuzbashyan, P. Silberzan, J. B. Stock, R. H. Austin, *Science*, 2003, 301, 188.
45 S. Park, P. M. Wolanin, E. A. Yuzbashyan, H. Lin, N. C. Darnton, P. Silberzan, J. B. Stock, R. H. Austin, *PNAS*, 2003, 100, 13910.

46 R. H. Austin, C-K. Tung, G. Lambert, D. Liao, X. Gong, *Chem. Soc. Rev.*, 2010, 39, 1049.